Journal of Catalysis **205,** 248–258 (2002)
doi:10.1006/jcat.2001.3459, available online at http://www.idealibrary.com on IDEAL®

Microcalorimetric Adsorption Characterizations of Supported Vanadia Catalysts for the Selective Oxidation of Propylene to Acetone

Mingshi Li and Jianyi Shen[1]

Department of Chemistry, Nanjing University, Nanjing 210093, China

Received May 4, 2001; revised October 22, 2001; accepted October 22, 2001; published online January 3, 2002

Structural characterizations and chemisorption of O_2 revealed that vanadium species in our 10% V_2O_5/TiO_2 and 10% V_2O_5/γ-Al_2O_3 catalysts were highly dispersed polyvanadates, while that in the 10% V_2O_5/SiO_2 was small-crystalline V_2O_5. Although the 10% V_2O_5/H–ZSM-5 exhibits strong Brønsted acidity that favors the adsorption of propylene, the poorly dispersed vanadium species makes it a poor catalyst for the conversion of propylene to acetone. The key factors determining the activity of the reaction are the number and strength of Brønsted acid sites of V–OH groups and the oxidation ability of oxidized vanadium species in the catalysts. The V_2O_5/TiO_2 catalyst exhibits the strongest Brønsted acidity of V–OH groups in the catalysts studied, and therefore it adsorbs propylene and shows the high activity for the conversion of propylene to acetone. In fact, Fourier transform infrared indicates that the adsorption of propylene on the V_2O_5/TiO_2 catalyst at room temperature leads to the formation of surface isopropoxy groups and adsorbed acetone. Both the 10% V_2O_5/γ-Al_2O_3 and 10% V_2O_5/SiO_2 catalysts possess weak Brønsted acidity of V–OH groups and therefore exhibit the low activity for the conversion of propylene to acetone. Microcalorimetric adsorption of reactants and products on the catalysts provides the information about the surface bonding strengths that may be used for the microkinetic analysis of the corresponding surface reactions. The initial heat for water adsorption on the V_2O_5/TiO_2 catalyst is lower than 90 kJ/mol, indicating that water is reversibly adsorbed at temperatures higher than 360 K. The heat of adsorption of acetone on the reduced V_2O_5/TiO_2 catalyst is about 100 kJ/mol, which can be used to estimate the activation energy for desorption of acetone from the catalyst. O_2 adsorption on the reduced catalysts produces high heat, indicating that the reoxidation of reduced vanadium species by O_2 is an irreversible reaction step.

Key Words: **oxidation of propylene to acetone; supported vanadia catalysts; microcalorimetric adsorption; surface acidity; bonding strengths of adsorbed surface species.**

1. INTRODUCTION

Ketones are commercially important and are usually produced by the dehydrogenation of corresponding alcohols (1). Since the alcohols can be obtained by the hydration of olefins, it would be more desirable to avoid the formation of intermediate products, alcohols, and to synthesize ketones by direct oxidation of olefins (2). It is well-known that ethylene can be oxidized by oxygen to acetaldehyde by the Wäker reaction in aqueous solution using the $PdCl_2$–$CuCl_2$ homogeneous catalyst. The problems with the Wäker process are that the catalyst is corrosive and that chlorinated side products may form. Since the formation of chlorinated side products is strongly enhanced when alkenes with more carbon atoms are used, the process has never been applied for the oxidation of higher alkenes, such as propylene, 1-butene, and 1-pentene. To overcome these problems encountered in the Wäker process, Stobbe-Kreemers *et al.* developed a heterogeneous catalyst, in which vanadium pentoxide (3) or heteropolyanions (4) were used to function as the redox sites in the heterogeneous process, as Cu(II)/Cu(I) do in the homogeneous process. Iwamoto and coworkers reported that ketones could be formed from lower olefins and water on ultrastable Y-type zeolite catalysts (5). Moro-oka and coworkers studied various binary oxide catalysts for the oxidation of propylene to acetone (6). They found that the SnO_2–MoO_3 binary catalyst showed the highest activity among the effective catalysts they studied. The metal oxide catalysts containing molybdenum were also effective for the oxidation of 1-butene and 1-pentene to methyl ethyl ketone and methyl propyl ketone, respectively (7). Recently, we found that a titania-supported vanadia catalyst exhibited the pronounced activity for the selective oxidation of propylene to acetone (8).

In this paper, we report the results of structural and surface acidity characterizations of the supported vanadia catalysts. The surface acidities were characterized using Fourier transform infrared (FTIR) and microcalorimetric adsorption of ammonia. In addition, microcalorimetric adsorption was used to probe the interactions of the reactants (propylene, oxygen, and water), the intermediate product (isopropanol), and the final product (acetone) with the supported vanadia catalysts for the oxidation of propylene to acetone. Accordingly, the catalytic performance can be correlated with the structure of vanadium species and acidities of the catalysts. The surface bond strengths of the related species as measured by the microcalorimetric adsorption

[1] To whom correspondence should be addressed. Fax: +86 25 3317761. E-mail: jyshen@nju.edu.cn.

0021-9517/02 $35.00

can be used for the initial estimation of activation energies of the elementary steps in modeling the reaction mechanism (9).

2. EXPERIMENTAL

2.1. Catalyst Preparation

Catalysts with 10 wt% V_2O_5 were prepared using the impregnation method. A solution containing oxalic acid and ammonium metavanadate was used for the impregnation. The supports used were H–ZSM-5 (350 m^2/g, $SiO_2/Al_2O_3 = 50$), SiO_2 (360 m^2/g), γ-Al_2O_3 (160 m^2/g), and TiO_2 (anatase, 53 m^2/g). The impregnated samples were first dried at 383 K and then calcined at 673 K. For comparison, a V_2O_5 sample was prepared by calcining ammonium metavanadate at 673 K for 4 h.

2.2. Determination of Vanadia Dispersion

The number of surface vanadium sites was titrated by O_2 adsorption at 640 K after the samples were reduced by H_2 at 640 K, according to the method developed by Oyama *et al.* (10). With the number of surface sites, the dispersion of vanadia in the supported catalysts and the reaction activity in turnover frequency (TOF) can be derived.

2.3. X-Ray Diffraction (XRD) and Diffuse Reflectance Spectroscopy (DRS)

X-ray diffractions were performed on a Rigaku D/Max-RA X-ray diffractometer equipped with a Cu target and graphite monochromator. The applied voltage and current were 40 kV and 80 mA, respectively. The scanning rate was 4°/min. DRS spectra were collected on a Shimadzu UV2100 UV–vis recording spectrophotometer at room temperature. The spectra were recorded against a halon white reflectance standard in the range of 900–190 nm.

2.4. Microcalorimetric Adsorption

The microcalorimetric adsorption measurements were performed using a Tian–Calvet type heat-flux calorimeter, which has been described in detail elsewhere (11, 12). The microcalorimetric adsorptions of O_2, H_2O, and NH_3 were carried out at 423 K while the microcalorimetric adsorptions of propylene, isopropanol, and acetone were performed at 313 K. The unreduced samples were pretreated *in situ* in O_2 at 673 K for 2 h and outgassed at 673 K for 1 h. The reduced samples were pretreated *in situ* in H_2 at 640 K for 2 h and outgassed at 640 K for 1 h. After thermal equilibrium was reached, the microcalorimetric data were collected by sequentially introducing small doses (usually 1–10 Torr, equivalent to 1–10 μmol) of probe molecules onto the sample until it became saturated (equilibrium pressure reached 5–6 Torr). The resulting heat response for each dose was recorded as a function of time and integrated to determine the energy released (mJ). The amount of gas adsorbed (μmol) was determined volumetrically by using a MKS Baratron capacitance manometer (accuracy: 0.001 Torr). The differential heat (kJ/mol), defined as the negative enthalpy change, was then calculated for each dose by dividing the heat released by the amount of gas adsorbed. The accuracy of differential heats was estimated to be within $\pm$5 kJ/mol (11).

2.5. FTIR Spectroscopy

The IR spectra were recorded with a Brucker IFS66V FTIR spectrophotometer. The sample treatments were the same as those for corresponding microcalorimetric adsorptions. A sample of about 10–15 mg was pressed to form a self-supporting pellet with the diameter of 13 mm. The IR cell was directly connected to a vacuum system equipped with a dosing section with known volume and a Baratron capacitance manometer (accuracy: 0.001 Torr), thus allowing quantitative dosing of probe molecules onto the pellet. After the pellet was properly treated, the spectrum of pellet was recorded as a background. Then about 3 Torr of adsorbate molecules (NH_3 or propylene) was dosed onto the pellet. Around 20 min after the dosing, the spectrum was collected again. The spectrum of adsorbed species was obtained by subtracting the background spectra for the pellet and gas-phase adsorbate from the spectrum of the pellet after dosing the adsorbate. All the spectra were collected in the absorbance mode at 4-cm^{-1} resolution, with 100 scans for adsorbed ammonia and 500 scans for adsorbed propylene.

2.6. Catalytic Activity

The catalytic test was carried out at 463 K at atmospheric pressure using 0.5 g of catalysts in a conventional flow microreactor connected online with a gas chromatograph. The flow rates of propylene, O_2, water vapor, and N_2 were 3.8, 6.3, 11, and 30 ml/min, respectively. The activity data were obtained at the steady state established in ca. 2 h. Afterward, no measurable loss of catalytic activity was observed up to 8 h on stream.

3. RESULTS AND DISCUSSION

3.1. Structural Characterization of the Catalysts

The results of vanadium dispersion for the catalysts measured by oxygen chemisorption at 640 K are given in Table 1. A titania-supported vanadia catalyst has the highest dispersion though its specific surface area is not high. The dispersion of vanadium in the catalysts follows the order $V_2O_5/TiO_2 > V_2O_5/\gamma$-$Al_2O_3 > V_2O_5/SiO_2 > V_2O_5$/H–ZSM-5, in agreement with the results reported in the literature (13).

TABLE 1

Surface Area and Dispersion of Supported Vanadia Catalysts

Catalyst	Loading of V_2O_5 (wt%)	Surface area ($m^2\ g^{-1}$)	Surface vanadium sites[a] (mmol g^{-1})	Density of sites (nm^{-2})	Vanadium dispersion (%)
V_2O_5/H–ZSM5	10	300	0.418	0.84	38.0
V_2O_5/SiO_2	10	298	0.580	1.17	52.7
V_2O_5/γ-Al_2O_3	10	164	0.719	2.64	65.5
V_2O_5/TiO_2	10	53	0.765	8.70	69.6

[a] It is assumed that the number of surface vanadium sites is equal to that of oxygen atoms adsorbed at 640 K on the reduced catalysts (10).

Figure 1 shows the XRD patterns of the supported vanadia catalysts. The pattern for small V_2O_5 crystallites (14) appeared for the SiO_2-supported sample but was not observed for the TiO_2- and γ-Al_2O_3-supported samples. This result is consistent with the O_2 chemisorption measurements that showed that the dispersion of vanadia on TiO_2 and γ-Al_2O_3 is much higher than on SiO_2.

The UV–vis diffuse reflectance spectra (DRS) are shown in Fig. 2. Absorption-edge energy in a DRS spectrum can be used to characterize the structure of supported vanadia (14). Specifically, the absorption edge shifts to higher energy with the increase in dispersion of vanadium. Thus, according to Fig. 2 and the assignment in the literature (14), the structure of vanadium in the TiO_2- and γ-Al_2O_3-supported catalysts is mainly dispersed polyvanadate while that on SiO_2 is similar to bulk V_2O_5.

3.2. Acidity Characterization

3.2.1. Acidity of catalysts. Microcalorimetric adsorption of NH_3 was used to determine the number and strength of surface acid sites on the catalysts. Figure 3 shows the results. The V_2O_5/H–ZSM-5 catalyst exhibits the strongest acidity with an initial heat of 170 kJ/mol and coverage of 1100 μmol/g for the adsorption of NH_3. Since the bulk vanadia exhibits very weak acidity and the dispersion of vanadia is low, the strong acidity of V_2O_5/H–ZSM-5 is apparently due to the Brønsted acid sites in the H–ZSM-5 support. The V_2O_5/TiO_2 catalyst exhibits an initial heat of 104 kJ/mol and coverage of 320 μmol/g for the adsorption of NH_3. The acidity of V_2O_5/TiO_2 may be attributed to the highly dispersed polyvanadate on the surface since either V_2O_5 or TiO_2 alone shows weak acidity. Topsøe also showed that V_2O_5/TiO_2 had a stronger acidity than did V_2O_5 (15). The adsorption of NH_3 on V_2O_5/SiO_2 produced the initial heat of 84 kJ/mol, indicating the relatively weak surface acidity of V_2O_5/SiO_2. This heat is close to that (100 kJ/mol) measured by Le Bars *et al.* for a 10% V_2O_5/SiO_2 catalyst (16). However, the saturation coverage of NH_3 on our V_2O_5/SiO_2 sample is quite high (550 μmol/g), indicating the presence of significant numbers of acid sites on this sample. These acid sites may be from the small V_2O_5 crystallites dispersed on SiO_2 since the SiO_2 support itself exhibited the very low NH_3 coverage of about 30 μmol/g (17). Figure 3 shows that V_2O_5/γ-Al_2O_3 exhibits an acidity stronger than that of V_2O_5/TiO_2, but weaker than that of the γ-Al_2O_3 support. Le Bars *et al.* also reported a lower heat for a 9.8% V_2O_5/γ-Al_2O_3 catalyst than for the γ-Al_2O_3 support using pyridine as the probe molecule (18).

FTIR spectra of NH_3 adsorbed on supported vanadia catalysts and γ-Al_2O_3 are shown in Fig. 4. The bands around 1393, 1450, and 1680 cm^{-1} can be assigned to ammonium cations produced by the interaction of ammonia with

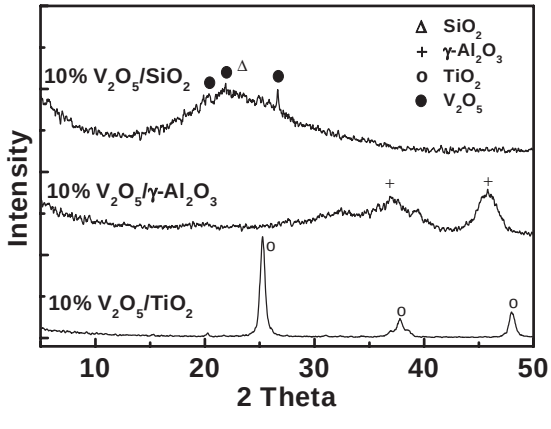

FIG. 1. XRD patterns of supported vanadia catalysts.

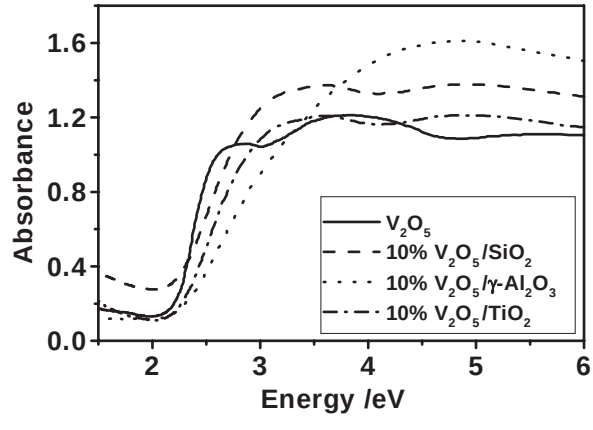

FIG. 2. Diffuse reflectance spectra of supported vanadia catalysts.

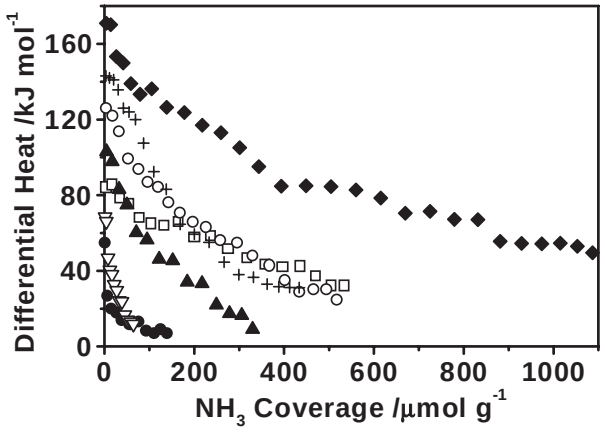

FIG. 3. Differential heat vs coverage for NH_3 adsorption at 423 K on 10% V_2O_5/H–ZSM-5 (◆), 10% V_2O_5/SiO_2 (□), 10% V_2O_5/γ-Al_2O_3 (○), 10% V_2O_5/TiO_2 (▲), bulk V_2O_5 (●), γ-Al_2O_3 (+), and TiO_2 (▽).

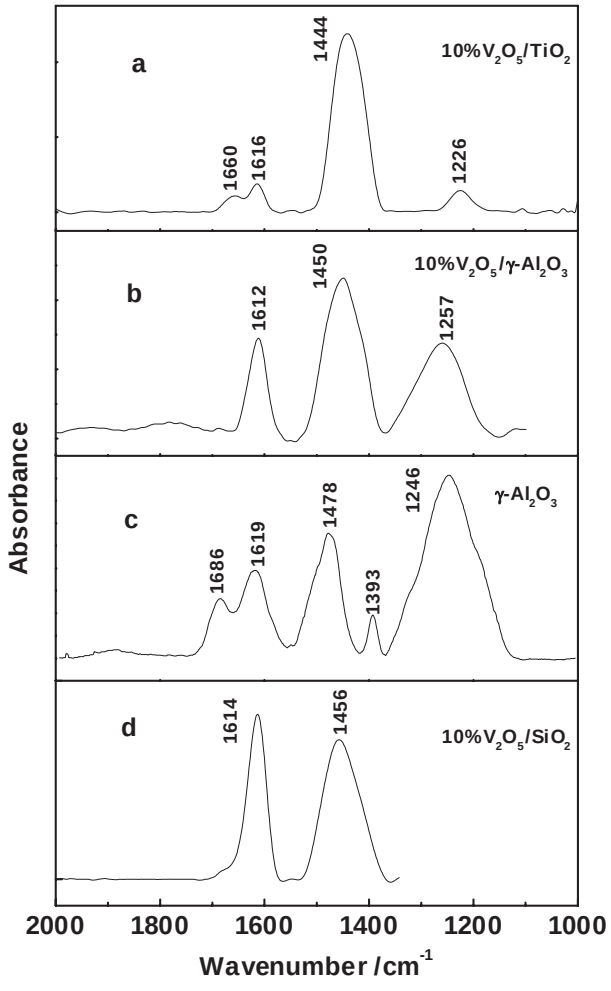

FIG. 4. FTIR spectra for NH_3 adsorption at room temperature on 10% V_2O_5/TiO_2 (a), 10% V_2O_5/γ-Al_2O_3 (b), γ-Al_2O_3 (c), and 10% V_2O_5/SiO_2 (d).

Brønsted acid sites while the bands around 1610 and 1230–1260 cm^{-1} are due to the coordinately adsorbed ammonia molecules on the Lewis acid sites (19, 20). Figure 4a is the IR spectrum collected for the V_2O_5/TiO_2 catalyst after ammonia adsorption. The main peak at 1444 cm^{-1} suggests that Brønsted acid sites dominate the surface of V_2O_5/TiO_2. This result agrees well with that reported in the literature (15). The two small peaks at 1616 and 1226 cm^{-1} indicate the existence of a small number of Lewis acid sites on the surface of the V_2O_5/TiO_2 catalyst.

The IR spectra for V_2O_5/γ-Al_2O_3 and γ-Al_2O_3 after ammonia adsorption are compared in Figs. 4b and 4c. It is seen that the main peak around 1478 cm^{-1} for Brønsted acid sites on γ-Al_2O_3 shifts to 1450 cm^{-1} for Brønsted acid sites on vanadia on addition of vanadia. In addition, the two peaks around 1686 and 1393 cm^{-1} for Brønsted acid sites on γ-Al_2O_3 disappeared. These results indicate an interaction of vanadium species with the surface Brønsted sites of γ-Al_2O_3. Furthermore, the relative intensity of the peak around 1260 cm^{-1} decreased, indicating that the vanadium species interact also with surface Lewis acid sites on γ-Al_2O_3. Thus, both Brønsted and Lewis acid sites are present on the surface of the V_2O_5/γ-Al_2O_3 catalyst. The Brønsted acid sites may be mainly from the surface vanadia, while the Lewis acid sites may be from surfaces of both the γ-Al_2O_3 support and supported vanadia. These results seem to be different from those reported by Le Bars *et al.* (18). They used a γ-Al_2O_3 that did not possess Brønsted acidity, as revealed by IR for pyridine adsorption. With the addition of vanadia, the Lewis acidity as evidenced by the band around 1449 cm^{-1} remained while the band at 1540 cm^{-1} for Brønsted acidity developed (18). Figure 4d shows that both Brønsted (1456 cm^{-1}) and Lewis (1614 cm^{-1}) acid sites are significantly present on the V_2O_5/SiO_2 catalyst. These two bands were negligible for NH_3 adsorption on the SiO_2 support since only hydrogen bonding can be formed between ammonia and surface hydroxyl groups on the SiO_2 support (21). Further IR measurements for the V_2O_5/SiO_2 catalyst after ammonia adsorption followed by evacuation at different temperatures indicate that Brønsted acid is stronger than Lewis acid on the V_2O_5/SiO_2 catalyst. It should be mentioned that our IR result for ammonia adsorption on the V_2O_5/SiO_2 catalyst does not agree with those reported by Le Bars *et al.*, where Brønsted acid sites were found to be the main surface acid sites over the V_2O_5/SiO_2 catalysts with different loadings (16).

Therefore, we obtained the following information by combining the results of microcalorimetry and FTIR for ammonia adsorption on supported vanadia catalysts. Vanadia supported on titania produces fairly strong acidity with an initial heat of 104 kJ/mol for ammonia adsorption. These acid sites are mainly Brønsted acid sites and may be attributed to V–OH groups of polyvanadate species highly

dispersed on titania. On the V_2O_5/γ-Al_2O_3 catalyst, the acid sites that are stronger than 104 kJ/mol may be Lewis acid sites from the support γ-Al_2O_3, while those weaker than that may be due to the V–OH groups that are Brønsted acid sites from the highly dispersed polyvanadate species. Both Brønsted and Lewis acid sites on the V_2O_5/SiO_2 catalyst are weak and are mainly produced by the small V_2O_5 crystallites dispersed on SiO_2.

3.2.2. Acidity of reduced catalysts. Microcalorimetric adsorption of NH_3 and FTIR for NH_3 adsorbed on the reduced samples were also performed in order to understand the effect of reduction on surface acidity of the supported vanadia catalysts. The samples were reduced *in situ* by H_2 at 640 K. The differential heat versus coverage for NH_3 adsorption on the reduced, unreduced, and propylene precovered V_2O_5/TiO_2 catalysts is shown in Fig. 5. It is seen that the strength and number of acid sites on V_2O_5/TiO_2 were decreased significantly on reduction. The IR spectra for NH_3 adsorption on the reduced and unreduced V_2O_5/TiO_2 catalysts are compared in Fig. 6. The peak around 1444 cm^{-1} was greatly diminished on reduction, indicating that the majority of surface V–OH groups acting as surface Brønsted acid sites were removed. The peak at 1226 cm^{-1} representing Lewis acid sites on vanadia now became a shoulder. A new peak appeared at 1156 cm^{-1}, which can be assigned to ammonia adsorbed on Lewis acid sites of TiO_2 (22). These results suggest that the surface of the original V_2O_5/TiO_2 catalyst was exclusively covered with the polyvanadate network. The reduction removes the surface V–OH groups, breaks the polyvanadate network, and exposes some areas of TiO_2 to the surface. Figure 5 shows that the preadsorption of propylene on the unreduced V_2O_5/TiO_2 catalyst resulted in a decrease in the initial heat for ammonia adsorption. The strength of the remaining acid sites was not changed by the preadsorption of propylene. This result seems to imply that propylene adsorbs only on Brønsted acid sites of the V_2O_5/TiO_2 catalyst that are stronger than 80 kJ/mol for ammonia adsorption.

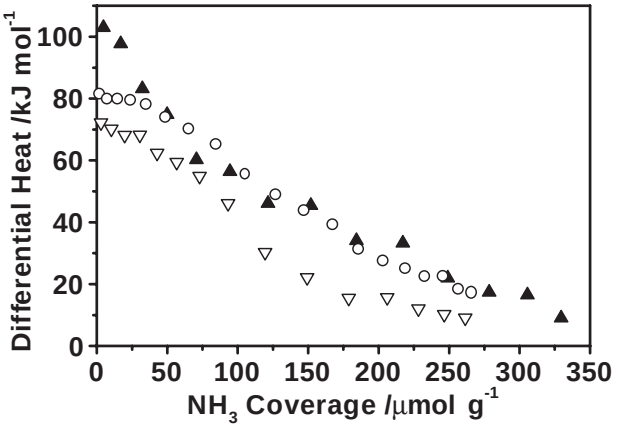

FIG. 5. Differential heat vs coverage for NH_3 adsorption at 423 K on unreduced (▲) and reduced (▽) 10% V_2O_5/TiO_2, and on propylene precovered unreduced 10% V_2O_5/TiO_2 (○).

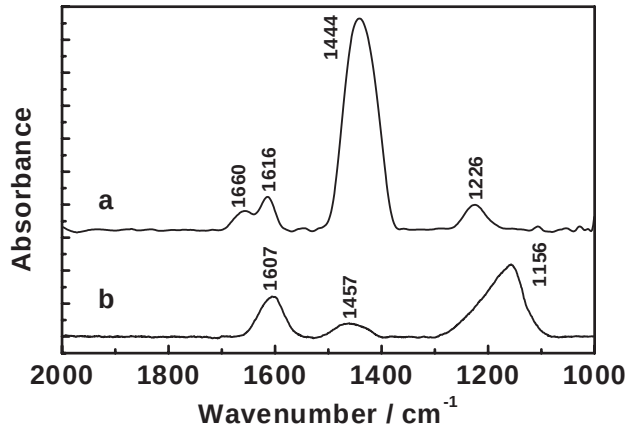

FIG. 6. FTIR spectra for NH_3 adsorption at room temperature on unreduced (a) and reduced (b) 10% V_2O_5/TiO_2.

3.2.3. Effect of water on acidity. Since the reaction for the conversion of propylene to acetone was performed in the presence of water, it should be desirable to study the effect of water on surface acidity of the catalysts. After it was cleaned by calcination at 673 K, the sample was cooled to 423 K, at which water vapor was dosed up to a saturation pressure of about 5–6 Torr. Then the sample was evacuated at 423 K for 0.5 h before ammonia adsorption. The results are shown in Fig. 7. It is seen that the preadsorption of water increased the strength of surface acidity for the V_2O_5/SiO_2 sample. This may be due to the fact that the adsorption of water converted some Lewis acid sites into Brønsted acid sites which are stronger acid sites on the V_2O_5/SiO_2 sample. In contrast, the addition of water on the V_2O_5/γ-Al_2O_3 catalyst decreased the strength of surface acidity. This may be due to the fact that some Lewis acid sites on the γ-Al_2O_3 support may be converted into Brønsted acid sites, which are weaker acid sites on γ-Al_2O_3. The preadsorption of water on the V_2O_5/TiO_2 catalyst almost did not alter the surface acidity, except for a significant increase in the initial heat for ammonia adsorption. Thus, the preadsorption of water may increase surface acidity of the V_2O_5/TiO_2 catalyst, which is favorable for the adsorption of propylene, which is the activation step for the reaction of selective oxidation of propylene to acetone.

3.3. Catalytic Activity

The reaction rates and TOFs of selective oxidation of propylene to acetone over the supported vanadia catalysts are listed in Table 2. All the catalysts exhibited high selectivity to acetone. The V_2O_5/TiO_2 catalyst showed the highest activity at 463 K, with the rate of acetone formation of 98 μmol g^{-1} min^{-1}, corresponding to a TOF of 2×10^{-3} s^{-1}. At first glance, the conversion of propylene

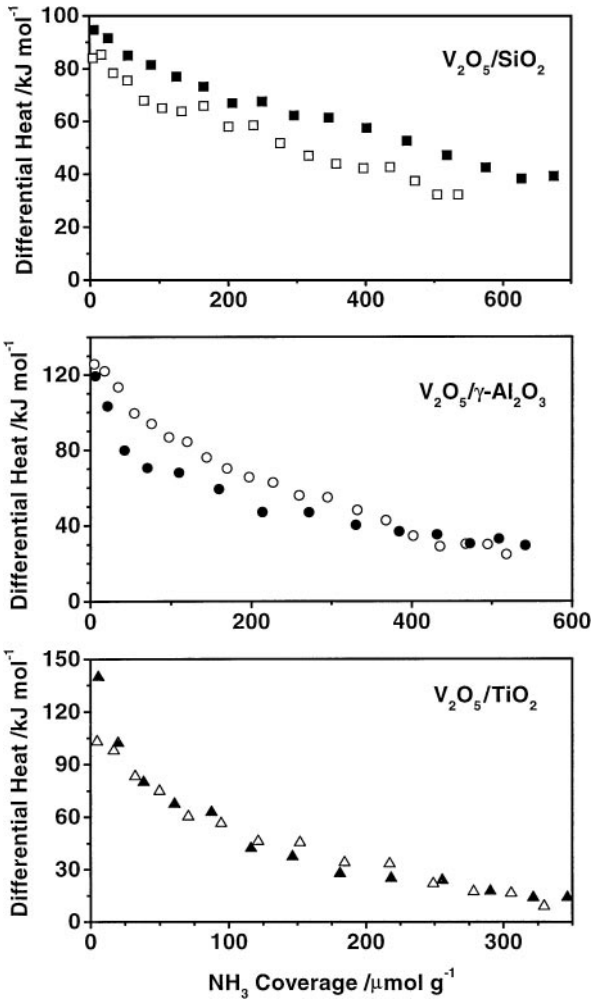

FIG. 7. Differential heat vs coverage for NH_3 adsorption at 423 K on 10% V_2O_5/SiO_2 (□), 10% V_2O_5/γ-Al_2O_3 (○), and 10% V_2O_5/TiO_2 (△), and on water precovered 10% V_2O_5/SiO_2 (■), 10% V_2O_5/γ-Al_2O_3 (●), and 10% V_2O_5/TiO_2 (▲).

seems to be related to the dispersion of vanadia on the different supports. In fact, both dispersion of vanadia and propylene conversion on the catalysts follow the order of $V_2O_5/TiO_2 > V_2O_5/\gamma$-$Al_2O_3 > V_2O_5/SiO_2 > V_2O_5$/H–ZSM-5. However, the activities in TOFs for these catalysts follow the same order. Thus, the correlation of activity with dispersion of vanadia does not provide insight into the chemistry of the catalytic reaction. The reaction mechanism (discussed in detail in Ref. 9) for the oxidation of propylene to acetone over vanadia catalysts may be expressed as follows:

$$V^{5+}\text{–O} + V^{3+} + H_2O \Leftrightarrow 2V^{4+}\text{–OH}, \quad [1]$$

$$V^{4+}\text{–OH} + CH_3CH{=}CH_2 \rightarrow V^{4+}\text{–O–CH}(CH_3)_2, \quad [2]$$

$$V^{4+}\text{–O–CH}(CH_3)_2 + V^{5+}\text{–O} \rightarrow V^{3+}\text{–O}{=}C(CH_3)_2 + V^{4+}\text{–OH}, \quad [3]$$

$$V^{3+}\text{–O}{=}C(CH_3)_2 \leftrightarrow CH_3COCH_3 + V^{3+}, \quad [4]$$

$$2V^{3+} + O_2 \rightarrow 2V^{5+}\text{–O}. \quad [5]$$

In this mechanism, propylene interacts with surface V–OH groups, which are the Brønsted acid sites, to form the isopropoxy species. Although V_2O_5/H–ZSM-5 exhibits the strongest Brønsted acidity of the catalysts studied, the dispersion of vanadium species on H–ZSM-5 is low, and therefore there must be few V–OH groups in this catalyst, so that it displays low activity for the conversion of propylene to acetone. The V_2O_5/γ-Al_2O_3 catalyst exhibited stronger acidity than the V_2O_5/TiO_2 catalyst. But the strong acidity in the V_2O_5/γ-Al_2O_3 is Lewis acidity and its Brønsted acidity is not strong. This is further discussed below using the microcalorimetric adsorption of propylene. In contrast, the V_2O_5/TiO_2 catalyst possesses substantial V–OH groups that are fairly strong Brønsted acid sites with the heat of 104 kJ/mol for ammonia adsorption. This may be one of the reasons why the V_2O_5/TiO_2 catalyst exhibited the highest activity for the conversion of propylene to acetone in these catalysts.

In order to understand the above mechanism and to obtain information about surface coverage and limiting steps, microkinetic analysis is needed and the results of the analyses have been presented in a separate paper (9). In this paper, we provide information about interaction energies for the reactants and products with the catalysts, which is essential for microkinetic analysis of the reaction.

TABLE 2

Rates and TOFs for Selective Oxidation of Propylene to Acetone over the Supported Vanadia Catalysts

Catalyst	Conversion of propylene[a] (mol%)	Selectivity of acetone (%)	Rate[b] (10^{-5} mol g^{-1} min^{-1})	TOF[c] (10^{-4} s^{-1})
V_2O_5/H–ZSM-5	1.1	92	0.36	1.37
V_2O_5/SiO_2	3.5	95	1.12	3.24
V_2O_5/γ-Al_2O_3	13	94	4.15	9.60
V_2O_5/TiO_2	31	93	9.78	21.31

[a] Reaction conditions: propylene, 3.8 ml/min; O_2, 6.3 ml/min; water (g), 13.5 ml/min; N_2, 30 ml/min; T = 463 K.
[b] Moles of acetone produced per gram of catalyst per minute.
[c] Number of acetone molecules produced per vanadium site per second.

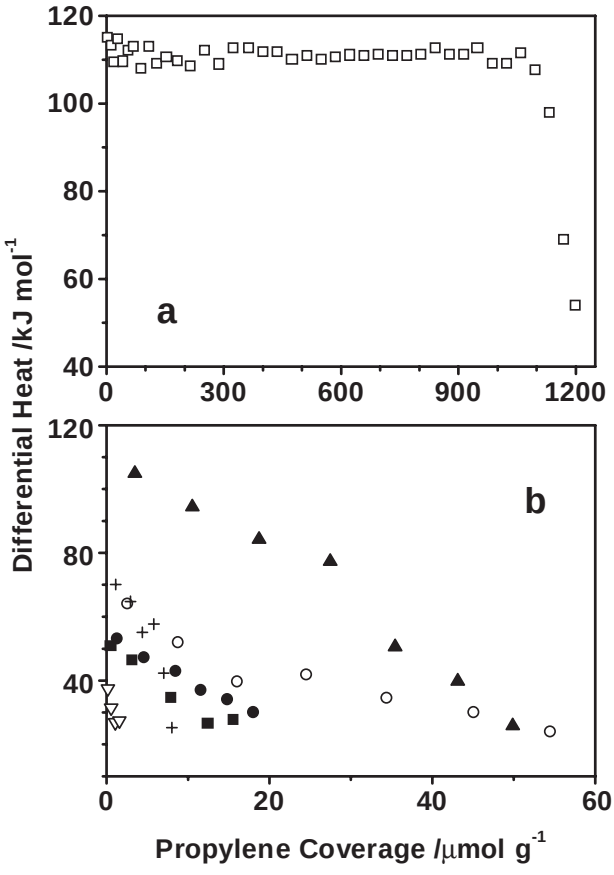

FIG. 8. Differential heat vs coverage for propylene adsorption at 313 K on 10% V_2O_5/H–ZSM-5 (□), 10% V_2O_5/SiO_2 (■), 10% V_2O_5/γ-Al_2O_3 (○), 10% V_2O_5/TiO_2 (▲), bulk V_2O_5 (▽), γ-Al_2O_3 (●), and TiO_2 (+).

3.4. Interactions of Reactants and Products with the Catalysts

3.4.1. Adsorption of propylene. Differential heat versus coverage for propylene adsorption on the catalysts at 313 K is shown in Fig. 8. As mentioned above, the dispersion of V_2O_5 on H–ZSM-5 is low. Thus, the high initial heat and coverage for the adsorption of propylene on V_2O_5/H–ZSM-5 (Fig. 8a) may be due to the interaction of propylene with surface protons of H–ZSM-5, which are strong Brønsted acid sites. It was reported that propylene oligomerizes when adsorbed on H–ZSM-5 (23). The oligomerization occurs via the reaction between adsorbed propylene (in the form of isopropoxy group) and gas-phase propylene. In our experimental conditions, oligomerization may not happen at the initial doses of propylene since the partial pressure of propylene was as low as ~1 Pa in this condition. The width of the peak (heat-flux signal) was small for the initial doses and peak broadening only occurred at the partial pressure of propylene of about 10 Pa and higher. Thus, the heat for the first doses of propylene may represent the interaction strength between propylene and the Brønsted acid sites in the H–ZSM-5 when oligomers were absent. Therefore, it may be concluded that the feasibility of protonation of propylene to form the isopropyl cations depends on the strength of the Brønsted acid sites. However, the activity of this catalyst for the conversion of propylene to acetone is low. These results imply that the strength of the Brønsted acid sites on V–OH is one of the key factors that determine the reaction activity.

Figure 8b shows that propylene is only weakly adsorbed on V_2O_5 and TiO_2. The adsorption of propylene on the V_2O_5/TiO_2 catalyst is substantially enhanced; the initial heat and coverage were measured to be 105 kJ/mol and 50 μmol/g, respectively. In this case, propylene molecules interact with surface V–OH groups to form surface isopropyl carbonium ions, which are then transformed into surface isopropoxy species on vanadia. The number and acid strength of surface V–OH groups on vanadia are significantly enhanced by the presence of TiO_2, as was confirmed as shown above, by the microcalorimetric adsorption of ammonia. Although the initial heat for the adsorption of propylene on the V_2O_5/γ-Al_2O_3 catalyst is low (64 kJ/mol), the coverage of propylene for this catalyst (55 μmol/g) is not low compared to that for V_2O_5/TiO_2. This implies that the strength of Brønsted acid sites of V–OH groups on V_2O_5/γ-Al_2O_3 is weaker than that on V_2O_5/TiO_2, while the strong acidity measured by the microcalorimetric adsorption of ammonia for the V_2O_5/γ-Al_2O_3 catalyst is due to Lewis acid sites on the γ-Al_2O_3 support. The similar coverage for the adsorption of propylene on V_2O_5/γ-Al_2O_3 and V_2O_5/TiO_2 indicates that the two catalysts may have a similar number of surface V–OH groups. The adsorption of propylene on the V_2O_5/SiO_2 catalyst is very weak in terms of adsorption heat and propylene coverage compared with that on the V_2O_5/TiO_2 and V_2O_5/γ-Al_2O_3 catalysts, owing to the poor dispersion of V_2O_5 on SiO_2 and the low acidity of Brønsted sites on the V_2O_5/SiO_2 catalyst.

The IR spectrum for the adsorption of propylene on the V_2O_5/TiO_2 catalyst at room temperature is shown in Fig. 9. Four bands were clearly observed around 1672, 1468, 1379, and 1096 cm^{-1}. The sharp band at 1096 cm^{-1} can be assigned to the stretching vibration of the C–O bond, indicating the formation of adsorbed isopropoxy species. The bands around 1468 and 1379 cm^{-1} belong to the bending vibration of CH_3 groups. The band around 1672 cm^{-1} is due to the stretching vibration of weakened C=O bond, indicating the formation of adsorbed acetone. Thus, the adsorption of propylene on V_2O_5/TiO_2 at room temperature produces mainly isopropoxy species with some adsorbed acetone. Molecular adsorbed propylene was not observed. This result is in agreement with what has been reported (24).

There is other evidence that propylene interacts with surface Brønsted acid sites of the vanadia catalysts. Figure 10 shows that the adsorption of propylene on the V_2O_5/TiO_2

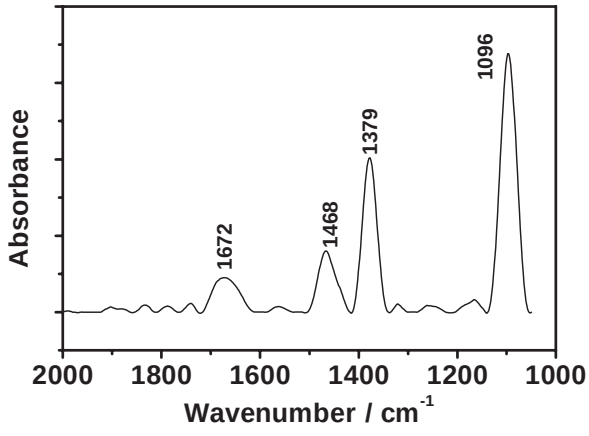

FIG. 9. FTIR spectrum for propylene adsorption on 10% V_2O_5/TiO_2 at room temperature.

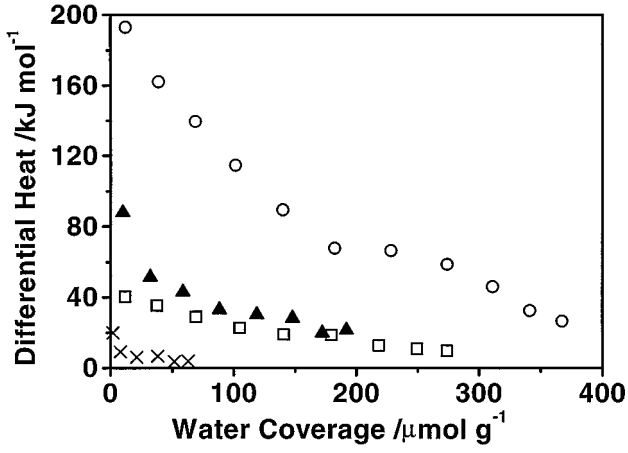

FIG. 11. Differential heat vs coverage for water adsorption at 423 K on 10% V_2O_5/SiO_2 (□), 10% V_2O_5/γ-Al_2O_3 (○), 10% V_2O_5/TiO_2 (▲), and bulk V_2O_5 (×).

catalyst was greatly diminished on the preadsorption of ammonia. Apparently, the preadsorbed ammonia molecules occupy V–OH groups to form ammonium cations and therefore prevent the interaction of propylene with V–OH groups. In addition, the adsorption of propylene on the reduced V_2O_5/TiO_2 catalyst was also significantly decreased, since the reduction resulted in a significant decrease in both number and strength of Brønsted acid sites on the V_2O_5/TiO_2 catalyst.

3.4.2. Adsorption of water. The differential heat versus coverage for water adsorption at 423 K on the supported vanadia catalysts are shown in Fig. 11. The adsorption of water on V_2O_5/γ-Al_2O_3 is strong with an initial heat of 193 kJ/mol and coverage of 370 μmol g^{-1}, respectively, which may be attributed to the adsorption of water on Lewis acid sites of the γ-Al_2O_3 support. The V_2O_5/SiO_2 catalyst and unsupported V_2O_5 adsorb water weakly with an initial heat of not higher than 40 kJ/mol. The adsorption of water on the V_2O_5/TiO_2 catalyst is not strong; the initial heat and coverage are 88 kJ/mol and 190 μmol g^{-1}, respectively. Thus, the adsorption of water on vanadia species in the V_2O_5/γ-Al_2O_3 catalyst may not be strong either. It is generally true that adsorption with a heat of less than 90 kJ/mol can be taken as reversible adsorption at temperatures higher than 360 K. Therefore, the adsorption of water on the V_2O_5/TiO_2 catalyst must be reversible at the reaction conditions. The difference of the activation energies for adsorption and desorption of water on V_2O_5/TiO_2 would be around 88 kJ/mol, which is the adsorption heat of water on the catalyst. This value can be used in modeling the reaction mechanism for the selective oxidation of propylene to acetone on the V_2O_5/TiO_2 catalyst (9).

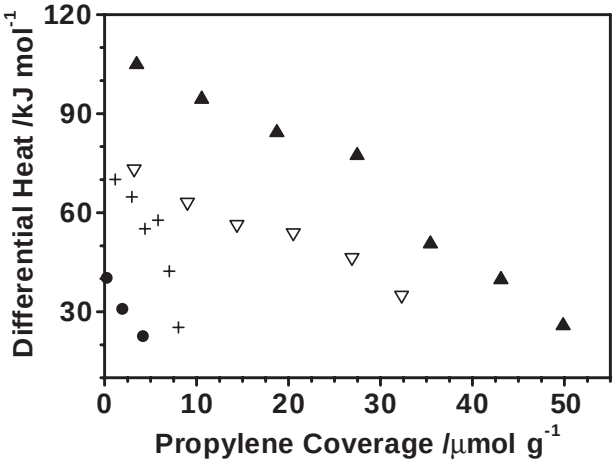

FIG. 10. Differential heat vs coverage for propylene adsorption at 313 K on 10% V_2O_5/TiO_2 (▲), NH_3 precovered 10% V_2O_5/TiO_2 (●), reduced 10% V_2O_5/TiO_2 (▽), and TiO_2 (+).

3.4.3. Adsorption of isopropanol. Isopropanol can be taken as the intermediate product for the selective oxidation of propylene to acetone. Thus, heat for the adsorption of isopropanol on the supported vanadia catalysts were measured. The differential heat versus coverage for the adsorption of isopropanol at 313 K on the unreduced and reduced vanadia catalysts are shown in Fig. 12. The strength of interaction of isopropanol with the unreduced catalysts is weak and follows the order V_2O_5/γ-$Al_2O_3 > V_2O_5/TiO_2 > V_2O_5/SiO_2$, which is the same order as the acidic strength of the unreduced catalysts. The adsorption of isopropanol on the unreduced V_2O_5/TiO_2 catalyst produced the initial heat of 53 kJ/mol. Thus, the adsorption of isopropanol on the unreduced V_2O_5/TiO_2 catalyst must be reversible and the difference for activation energies of desorption and adsorption of isopropanol on V_2O_5/TiO_2 would be around 53 kJ/mol. This value can be used for modeling the reaction mechanism for the conversion of isopropanol to acetone over the V_2O_5/TiO_2 catalyst (9). It is interesting to note that the adsorption of

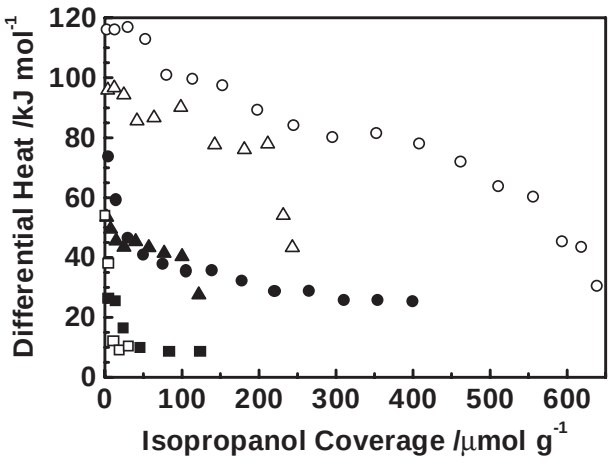

FIG. 12. Differential heat vs coverage for isopropanol adsorption at 313 K on unreduced 10% V_2O_5/SiO_2 (■), 10% V_2O_5/γ-Al_2O_3 (●), and 10% V_2O_5/TiO_2 (▲), as well as on reduced 10% V_2O_5/SiO_2 (□), 10% V_2O_5/γ-Al_2O_3 (○), and 10% V_2O_5/TiO_2 (△).

isopropanol is greatly enhanced on the reduced catalysts. For example, the initial heat for isopropanol adsorption on the V_2O_5/TiO_2 and V_2O_5/γ-Al_2O_3 catalysts was increased from 53 to 95 kJ/mol and from 74 to 115 kJ/mol, respectively, on reduction. The coverage of isopropanol on these two catalysts was also substantially increased on reduction. This can be explained by the fact that the reduction resulted in an increase in Lewis acid sites on the catalysts, as can be seen in Fig. 6 for the V_2O_5/TiO_2 catalyst. The dissociative adsorption of isopropanol requires the coordinately unsaturated vanadium sites for accommodation of the formed isopropoxy groups. The process can be expressed as (9)

$$\begin{aligned} &CH_3CH(OH)CH_3 + V^{3+} + V^{5+}\text{–}O \\ &\quad \rightarrow V^{3+}\text{–}O\text{–}CH(CH_3)_2 + V^{5+}\text{–}OH \\ &\quad \Leftrightarrow V^{4+}\text{–}O\text{–}CH(CH_3)_2 + V^{4+}\text{–}OH, \end{aligned}$$

where V^{5+}–O represents the oxidation sites while V^{3+} is the oxygen-deficient sites. In this equation, it is assumed that a rapid electron charge exchange might occur between the vanadium sites with different valent states because of the semiconductor nature of vanadium oxide species (25):

$$V^{5+}\text{–}O + V^{3+} \Leftrightarrow V^{4+}\text{–}O + V^{4+}$$

3.4.4. Adsorption of acetone. Desorption of acetone is an elementary step in the reaction mechanism. The microcalorimetric adsorption of acetone has been used to provide information about the strength of acetone adsorbed on the supported vanadia catalysts. Figure 13a shows the plots of the differential heat versus coverage for acetone adsorption at 313 K on the γ-Al_2O_3, TiO_2, and supported vanadia catalysts. The adsorption of acetone on γ-Al_2O_3 is quite strong with an initial heat of 115 kJ/mol and coverage of as high as 1000 μmol g^{-1}, owing to acetone adsorption on strong Lewis acid sites of γ-Al_2O_3. The addition of V_2O_5 onto the γ-Al_2O_3 greatly weakens acetone adsorption, owing to the decrease in number and strength of surface Lewis acid sites on γ-Al_2O_3. The adsorption of acetone on TiO_2 support is weak, indicating weak Lewis acidity of TiO_2. The addition of V_2O_5 onto TiO_2 significantly enhances the adsorption of acetone, indicating an increase in Lewis acidity. Although the initial heat for acetone adsorption on V_2O_5/SiO_2 is lower than that on V_2O_5/TiO_2, the acetone coverage is much higher on V_2O_5/SiO_2, revealing the existence of a substantial number of Lewis acid sites on the V_2O_5/SiO_2 catalyst, and agreeing well with the above IR result for ammonia adsorption on the catalyst. Figure 13b shows the effects of reduction and preadsorption of water on the adsorption of acetone on the V_2O_5/TiO_2 catalyst. It is seen that the reduction significantly enhances adsorption of acetone on the V_2O_5/TiO_2 catalyst. The reason is apparent. The reduction significantly increases the number of surface Lewis acid sites on the V_2O_5/TiO_2 catalyst. Since the desorption of acetone results in the appearance of reduced vanadium species (or oxygen-deficient sites), as shown by

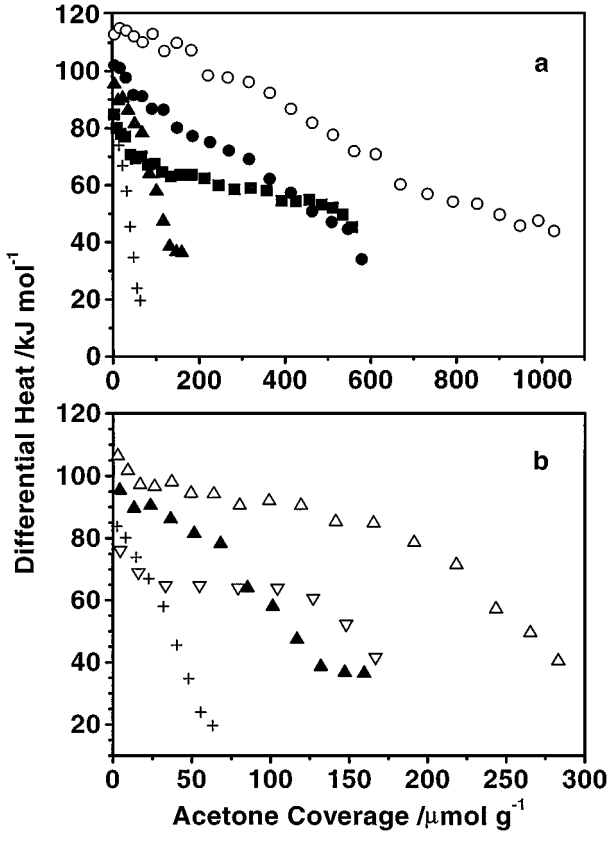

FIG. 13. Differential heat vs coverage for acetone adsorption at 313 K on unreduced 10% V_2O_5/SiO_2 (■), 10% V_2O_5/γ-Al_2O_3 (●), and 10% V_2O_5/TiO_2 (▲), on reduced 10% V_2O_5/TiO_2 (△), and on reduced and water precovered 10% V_2O_5/TiO_2 (▽), γ-Al_2O_3 (○), and TiO_2 (+).

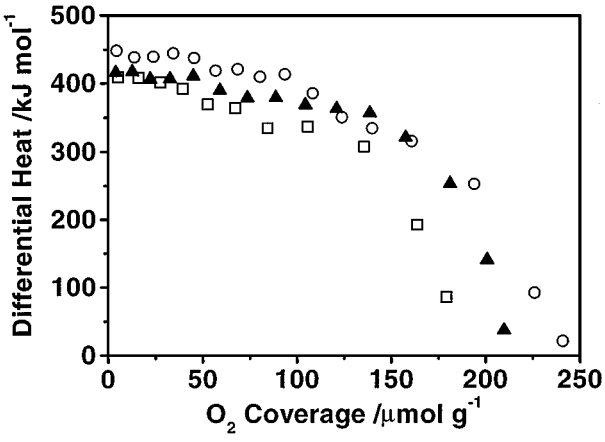

FIG. 14. Differential heat vs coverage for oxygen adsorption at 423 K on reduced 10% V_2O_5/SiO_2 (□), 10% V_2O_5/γ-Al_2O_3 (○), and 10% V_2O_5/TiO_2 (▲).

step [4] in the mechanism, the heat for acetone adsorption on the reduced V_2O_5/TiO_2 catalyst may be used to estimate the activation energy for the desorption of acetone from the V_2O_5/TiO_2 catalyst. When the reduced V_2O_5/TiO_2 catalyst was precovered by water, both initial heat and coverage for acetone adsorption decreased greatly. Thus, the presence of water may promote desorption of acetone from the reduced V_2O_5/TiO_2 catalyst.

3.4.5. Adsorption of oxygen. It has been shown that the surface V^{5+}–O species can be reduced to V^{3+} by H_2 at 640 K (10). The coordinately unsaturated V^{3+} species can then be reoxidized by O_2 to V^{5+}–O. The heat for this oxidation can be used to estimate the strength of V^{5+}–O bond. Figure 14 shows the results of microcalorimetric adsorption of O_2 at 423 K on the V_2O_5/SiO_2, V_2O_5/γ-Al_2O_3, and V_2O_5/TiO_2 catalysts prereduced by H_2 at 640 K. The heat for O_2 adsorption on the reduced catalysts is approximately the same (415–445 kJ/mol). The high heats suggest that the reoxidation of reduced vanadium sites by O_2, which is step [5] in the mechanism, should be irreversible.

4. CONCLUSIONS

The dispersion and surface structure of SiO_2, γ-Al_2O_3, TiO_2 (anatase), and H–ZSM-5 supported vanadia catalysts have been investigated by chemisorption of O_2, XRD, and DRS. It was found that vanadium species in the 10% V_2O_5/TiO_2 and 10% V_2O_5/γ-Al_2O_3 catalysts were highly dispersed polyvanadates, while that in the 10% V_2O_5/SiO_2 catalyst was small-crystalline V_2O_5. Microcalorimetric and infrared spectroscopic measurements for NH_3 adsorption revealed that the V_2O_5/TiO_2 catalyst possessed fairly strong Brønsted acidity due to surface V–OH groups (104 kJ/mol for NH_3 adsorption) with little surface Lewis acidity. The reduction significantly decreased the acid strength and number of Brønsted acid sites related to V–OH, but increased Lewis acid sites related to TiO_2 for the V_2O_5/TiO_2 catalyst. This result indicated that a polyvanadate network originally covered the surface of the V_2O_5/TiO_2 catalyst. The addition of vanadia to γ-Al_2O_3 decreased surface acid strength and the number of surface Lewis acid sites associated with γ-Al_2O_3 and increased the surface Brønsted acid sites related to V–OH groups. The V_2O_5/SiO_2 sample exhibited weak surface acidity (84 kJ/mol for NH_3 adsorption) and might possess similar numbers of Brønsted and Lewis acid sites.

The 10% V_2O_5/H–ZSM-5 catalyst exhibited strong Brønsted acidity that favored the adsorption of propylene, but the poorly dispersed vanadium species made it a poor catalyst for the conversion of propylene to acetone. The adsorption of propylene on Brønsted acid sites of dispersed vanadium species may be a key step for the reaction. The V_2O_5/TiO_2 catalyst exhibited the strongest Brønsted acidity of V–OH groups in the catalysts studied, and therefore it adsorbed propylene substantially and showed high activity for the conversion of propylene to acetone. In fact, FTIR indicated that the adsorption of propylene on the V_2O_5/TiO_2 catalyst at room temperature led to the formation of surface isopropoxy groups and adsorbed acetone. Both the 10% V_2O_5/γ-Al_2O_3 and the 10% V_2O_5/SiO_2 catalysts possessed weak Brønsted acidity of V–OH groups and therefore exhibited low activity for the conversion of propylene to acetone.

Microcalorimetric adsorption of reactants and products on the catalysts provided information about the surface bonding strengths that may be used for microkinetic analysis of the surface reactions. Water did not adsorb strongly on the V_2O_5/TiO_2 catalyst. The initial heat was determined to be lower than 90 kJ/mol, indicating that water may be reversibly adsorbed on the V_2O_5/TiO_2 catalyst at temperatures higher than 360 K. Isopropanol can be taken as an intermediate product of the reaction. Adsorption of isopropanol on the unreduced vanadia catalysts produced the initial heat lower than 75 kJ/mol. Reduction of the catalysts produced Lewis acid sites and enhanced greatly the adsorption of isopropanol. Acetone adsorbs on Lewis acid sites, too. Thus, the coverage of acetone on the V_2O_5/γ-Al_2O_3 and V_2O_5/SiO_2 catalysts was measured to be about 600 μmol/g, while that on V_2O_5/TiO_2 was found to be only about 170 μmol/g. Reduction of the V_2O_5/TiO_2 catalyst increased the coverage of acetone to about 300 μmol/g, because of the significant production of Lewis acid sites. The heat of adsorption of acetone on the reduced 10% V_2O_5/TiO_2 catalyst was determined to be about 100 kJ/mol, which can be used to estimate the activation energy for desorption of acetone from the catalyst. O_2 adsorption on the reduced catalysts produced high heat, demonstrating that the reoxidation of reduced vanadium species by O_2 should be an irreversible reaction step.

ACKNOWLEDGMENTS

This work is supported by the National Natural Science Foundation of China (grant 29973013) and the Department of Science and Technology of China (grant G1999022408). Financial support from the "333" project of Jiangsu Province is also acknowledged.

REFERENCES

1. Misono, M., and Nojiri, N., *Appl. Catal.* **64**, 1 (1990).
2. Mochida, I., Hayata, S., Kato, A., and Seiyama, T., *Bull. Chem. Soc. Jpn.* **44**, 2282 (1971).
3. Stobbe-Kreemers, A. W., Makkee, M., and Scholten, J. J. F., *Appl. Catal.* **156**, 219 (1997).
4. Stobbe-Kreemers, A. W., Dielis, R. B., Makkee, M., and Scholten, J. J. F., *J. Catal.* **154**, 175 (1995).
5. Mori, H., Ueno, H., Mizuno, N., Yahiro, H., and Iwamoto, M., *Chem. Lett.* **228**, 2289 (1990).
6. Moro-oka, Y., Takita, Y., and Ozaki, A., *J. Catal.* **23**, 183 (1971).
7. Tan, S., Moro-oka, Y., and Ozaki, A., *J. Catal.* **17**, 132 (1970).
8. Li, M., and Shen, J., *React. Kinet. Catal. Lett.* **72**, 263 (2001).
9. Li, M., Shen, J., and Lei, Y., *J. Catal.*, submitted.
10. Oyama, S. T., Went, G. T., Lewis, K. B., Bell, A. T., and Somorjai, G. A., *J. Phys Chem.* **93**, 6786 (1989).
11. Handy, B. H., Sharma, S. B., Spiewak, B. E., and Dumesic, J. A., *Meas. Sci. Technol.* **4**, 1350 (1993).
12. Cardona-Martinez, N., and Dumesic, J. A., *Adv. Catal.* **38**, 149 (1992).
13. Went, G. T., Oyama, S. T., and Bell, A. T., *J. Phys Chem.* **94**, 4240 (1990).
14. Khodakov, A., Olthof, B., Bell, A. T., and Iglesia, E., *J. Catal.* **181**, 205 (1999).
15. Topsøe, N. Y., *J. Catal.* **128**, 499 (1991).
16. Le Bars, J., Vedrine, J. C., Auroux, A., Trautmann, S., and Baerns, M., *Appl. Catal. A* **88**, 179 (1992).
17. Shen, J., Lochhead, M. J., Bray, K. L., Chen, Y., and Dumesic, J. A., *J. Phys. Chem.* **99**, 2384 (1995)
18. Le Bars, J., Vedrine, J. C., Auroux, A., Trautmann, S., and Baerns, M., *Appl. Catal. A* **119**, 341 (1994).
19. Shen, J., Cortright, R. D., Chen, Y., and Dumesic, J. A., *J. Phys. Chem.* **98**, 8607 (1994).
20. Knözinger, H., *Adv. Catal.* **25**, 186 (1976).
21. Rajadhyaksha, R. A., and Knözinger, H., *Appl. Catal.* **51**, 81 (1989).
22. Busca, G., Saussey, H., Saur, O., Lavalley, J. C., and Lorenzelli, V., *Appl. Catal.* **14**, 245 (1985).
23. Haw, J. F., Richardson, B. R., Oshiro, I. S., Lazo, N. D., and Speed, J. A., *J. Am. Chem. Soc.* **111**, 2052 (1989).
24. Escribano, V. S., Busca, G., and Lorenzelli, V., *J. Phys. Chem.* **94**, 8939 (1990).
25. Pomonis, P. J., and Vickerman, J. C., *Faraday Discuss. Chem. Soc.* **72**, 247 (1981).